

8. Jung, O.-S.; Pierpont, C. G. *J. Am. Chem. Soc.* **1994**, *116*, 1127.
9. Jung, O.-S.; Pierpont, C. G. *J. Am. Chem. Soc.* **1994**, *116*, 2229.
10. Pierpont, C. G.; Jung, O.-S. *Inorg. Chem.* **1995**, *34*, 4281.
11. Bosserman, P. J.; Sawyer, D. T. *Inorg. Chem.* **1982**, *21*, 1545.
12. Stallings, M. D.; Morrison, M. M.; Sawyer, D. T. *Inorg. Chem.* **1981**, *20*, 2655.
13. Bodini, M. E.; Copia, G.; Robison, R.; Sawyer, D. T. *Inorg. Chem.* **1983**, *22*, 126.
14. Jones, T. E.; Chin, D.-H.; Sawyer, D. T. *Inorg. Chem.* **1981**, *20*, 4257.
15. Jones, T. E.; Leon, L. E.; Sawyer, D. T. *Inorg. Chem.* **1982**, *21*, 3692.
16. Zirong, D.; Bhattacharya, S.; McCusker, J. K.; Hagen, P. M.; Hendrickson, D. N.; Pierpont, C. G. *Inorg. Chem.* **1992**, *31*, 870.
17. Attia, A. S.; Conklin, B. J.; Lange, C. W.; Pierpont, C. G. *Inorg. Chem.* **1996**, *35*, 1033.
18. Jung, O.-S.; Park, S. H.; Lee, Y.-A.; Chae, H. K.; Sohn, Y. S. *Bull. Korean Chem. Soc.* **1996**, *17*, 1085.
19. Snyder, H. R. *J. Am. Chem. Soc.* **1946**, *68*, 1204.
20. Belostotskaya, I. S.; Komissarova, N. L.; Dzhuraryan, E. V.; Ershov, V. V. *Izv. Akad. Nauk, SSSR*, **1972**, 1594.

## Energy Transfer from Gd<sup>3+</sup> to Eu<sup>3+</sup> in (Y, Gd)BO<sub>3</sub>:Eu<sup>3+</sup>

Yong Yune Shin, Youngrag Do<sup>†</sup>, and Youhyuk Kim\*

*Department of Chemistry and Information Display Research Center, Dankook University, Cheonan, Choongnam 330-714, Korea*

<sup>†</sup>*Samsung Display Device Co. Ltd. 575 Shin-Dong, Paldal-Gu, Suwon, Kyungki-Do 442-390, Korea*

*Received April 15, 1997*

Phosphors comprising rare-earth borate activated by rare earth ions have been neglected in the past, partly because of their lack of applicability to the field of display panels. Recently, however, some phosphors based on rare-earth borate have been used in color plasma display panel (PDP) which is the most promising flat display for the large area display.<sup>1</sup> Phosphors used in PDP are excited with vacuum ultraviolet radiation (147, 172 nm) from a Penning mixtures (Ne+Xe) in the panel. Naturally the phosphors are required to have a good quantum efficiency in the region below 200 nm. In this context rare-earth borates which give intense absorption peaks in this region have been selected as suitable host materials in PDP phosphors.<sup>2</sup> One of efficient red phosphors in PDP is a (Y, Gd)BO<sub>3</sub>:Eu, which contains two components in the host lattice.

Based on previously investigated metal oxide systems, which show an energy transfer from pair Gd ions to other RE<sup>3+</sup>,<sup>3</sup> gadolinium ions in the (Y, Gd)BO<sub>3</sub>:Eu<sup>3+</sup> are expected to transfer an absorbed energy to Eu<sup>3+</sup>. We have investigated luminescence properties of (Y, Gd)BO<sub>3</sub>:Eu as a function of Eu<sup>3+</sup> and Gd<sup>3+</sup> to elucidate the role of gadolinium ions in this phosphor.

### Experimental

Phosphors with the general formula [(Y<sub>0.9</sub>, Gd<sub>0.1</sub>)<sub>1-x</sub>Eu<sub>x</sub>]BO<sub>3</sub> (x=0.01-0.2), [(Y<sub>0.9</sub>, Eu<sub>0.1</sub>)<sub>1-x</sub>Gd<sub>x</sub>]BO<sub>3</sub> (x=0.01-0.7) and (Y<sub>0.9-x</sub>Gd<sub>x</sub>)BO<sub>3</sub>:Eu<sub>0.1</sub> (x=0-0.9) were prepared by the usual solid-state reaction.<sup>4</sup> The exact compositions of the phosphors are described in the text whenever such descriptions are necessary. The properties of phosphors are generalized

and do not pertain to one specific phosphor composition.

The raw materials Y<sub>2</sub>O<sub>3</sub>, Gd<sub>2</sub>O<sub>3</sub>, Eu<sub>2</sub>O<sub>3</sub> and H<sub>3</sub>BO<sub>3</sub> were thoroughly mixed with a small amount of a flux. The mixture was then charged in an alumina crucible with an alumina lid and fired at 1100 °C for 2h. Of the raw materials, Y<sub>2</sub>O<sub>3</sub> (Molycorp) and Eu<sub>2</sub>O<sub>3</sub> (Molycorp) were at 99.99% purity and Gd<sub>2</sub>O<sub>3</sub> (ShinEtsu) was 99.9% purity. The other raw materials were of reagent grade.

The phosphors were characterized by X-ray diffraction analysis. The excitation spectra between 200 and 400 nm were obtained with a Filter OG530 on excitation slit 0.28 mm and emission slit 0.9 mm by a home-made spectrofluorimeter (monochromator:ORIEL, light source:ORIEL 150W, detector:HAMAMATUS R-928) at KIST in Seoul. The emission spectra between 400 and 700 nm were obtained with a 254 nm excitation wavelength by a Samsung optical spectra multichannel analyzer (OSMA). For selective irradiation, the emission spectra were collected by a home-made spectrofluorimeter at Samsung Co. in Suwon as a function of excitation wavelength.

### Results and Discussion

Prepared powders of (Y, Gd)BO<sub>3</sub>:Eu<sup>3+</sup> show a single phase which corresponds to a solid solution on all the powder patterns. This is expected by a similarity of the crystal ionic radii of Y<sup>3+</sup> (0.93Å), Gd<sup>3+</sup> (0.94Å) and Eu<sup>3+</sup> (0.95Å).<sup>5</sup> The replacement of Y<sup>3+</sup> ions with Gd<sup>3+</sup> and Eu<sup>3+</sup> ions is, therefore, easily occurred to give a solid solution.

**Excitation Spectra.** Figure 1 shows the excitation spectra of various compositions of (Y<sub>0.9-x</sub>Gd<sub>x</sub>)BO<sub>3</sub>:Eu<sub>0.1</sub> ranging from 200 to 425 nm with the emission line at 593 nm. The concentration of activator, Eu<sup>3+</sup> maintains a con-

\*To whom all correspondence should be addressed.

stant level. The excitation spectrum of  $Y_{0.9}BO_3:Eu_{0.1}$  which is prepared by the solid state reaction is shown in Figure 1 (a). This spectrum can be used as a reference for comparison with other phosphors containing  $Gd^{3+}$  ion.

The excitation spectrum of Figure 1 (a) consists of a broad band at 245 nm corresponding to the charge transfer band of  $YBO_3:Eu^{3+}$  and a number of lines which could be assigned to the direct excitation transitions within the  $4f^6$  configuration of  $Eu^{3+}$  for 280-425 nm.

When a 0.2 mole fraction of gadolinium is incorporated into the host lattice, new peaks at 276, 308 and 314 nm appears as shown in Figure 1 (b). The relative intensities of these new peaks increase with increasing  $Gd^{3+}$  concentration as illustrated in Figure 1 (c), (d) and (e). These new peaks are, therefore, assigned due to the direct excitation of  $Gd^{3+}$ . The excitation line at 314 nm is assigned as the transition  $^8S_{7/2} \rightarrow ^6P_{5/2}$  and the line at 308 nm is the transition  $^8S_{7/2} \rightarrow ^6P_{5/2}$ . Other line could be assigned to the transition  $^8S_{7/2} \rightarrow ^6I_{9/2} + ^6I_{7/2}$  for 276 nm. Similar assignment has been found in  $Y_2O_3:Gd^{3+}$ .<sup>3</sup> Other transitions due to  $Gd^{3+}$ , namely  $^8S_{7/2} \rightarrow ^6D_{7/2}$ ,  $^6D_{5/2}$  and  $^6D_{3/2}$  seem to be buried under the broad band at 250 nm. The dependence of  $Gd^{3+}$  on the excitation spectrum indicates that the role of gadolinium in  $(Y, Gd)BO_3:Eu^{3+}$  is to transfer excitation energy to the emitting center,  $Eu^{3+}$ . Similar behavior has been reported by Ropp in  $(Y, Gd)_2O_3:Eu^{3+}$ .<sup>6</sup>

**Emission Spectra.** Figure 2 shows a typical emission spectrum of  $(Y, Gd)BO_3:Eu^{3+}$  phosphors excited by a 254 nm irradiation. The Spectrum of Figure 2 consists of several intense lines in the range of 590-630 nm. The maximum emission peak is located at 593 nm. Luminescence lines at 593, 612 (and 627) nm are assigned to the transitions of  $^5D_0$

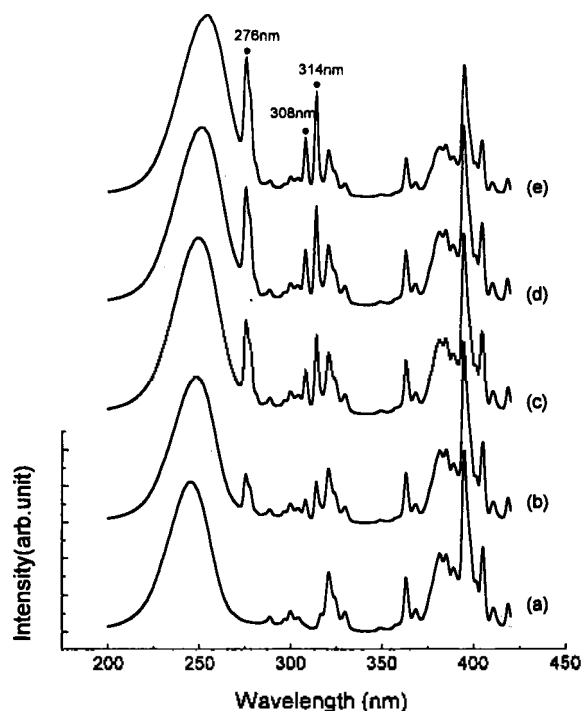


**Figure 1.** Excitation spectra of  $(Y_{0.9-x}Gd_x)BO_3:Eu_{0.1}$ ; (a)  $x=0$ , (b) 0.2, (c) 0.4, (d) 0.6, (e) 0.8, ● represents peaks due to gadolinium ions ( $\lambda_{em}=593$  nm).

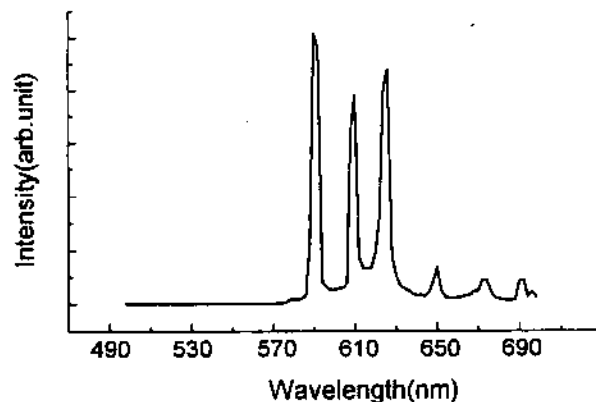


**Figure 2.** Emission spectrum of  $[(Y, Gd)_{0.85}]BO_3:Eu_{0.15}$  ( $Y:Gd=9:1$ ,  $\lambda_{exc}=254$  nm).

$\rightarrow ^7F_1$  and  $^5D_0 \rightarrow ^7F_2$ , respectively. This spectrum shows different features with that of  $Y_2O_3:Eu^{3+}$ , which has a dominant hypersensitive forced electric dipole emission in the  $^5D_0 \rightarrow ^7F_2$  transition.<sup>7</sup> This difference seems to be due to an  $Eu^{3+}$  site symmetry.

The dependence of the  $Eu^{3+}$  luminescence on gadolinium concentration has also been observed. The variation of luminescence intensities at 593 nm in  $(Y_{0.9-x}Gd_x)BO_3:Eu_{0.1}$  is plotted in Figure 3 as a function of gadolinium concentration. As the gadolinium content increases, relative intensities of peaks are also increased. This shows that the absorbed energy by  $Gd^{3+}$  is transferred to  $Eu^{3+}$  with a large range of gadolinium. The energy transfer efficiency of  $Gd^{3+}$  can be represented by the luminescence intensity of the  $Eu^{3+}$ . The optimum gadolinium concentration for the energy transfer is, therefore, around a 0.7 mole fraction of  $GdBO_3$  in  $(Y, Gd)BO_3:Eu_{0.1}$ . Above a 0.7 mole fraction of  $GdBO_3$  in Figure 3 the relative intensity of emission line at 593 nm starts to decrease.

**Concentration Quenching.** To observe concentration quenching<sup>8</sup> due to europium activator and conform the energy transfer from gadolinium to europium further, selective irradiation experiments at 255, 277 and 320 nm were performed at compositions of  $[(Y_{0.9-x}Gd_x)_{1-x}]BO_3:Eu_{0.1}$  ( $x=0.01-0.2$ ). To prevent the contribution of gadolinium, the

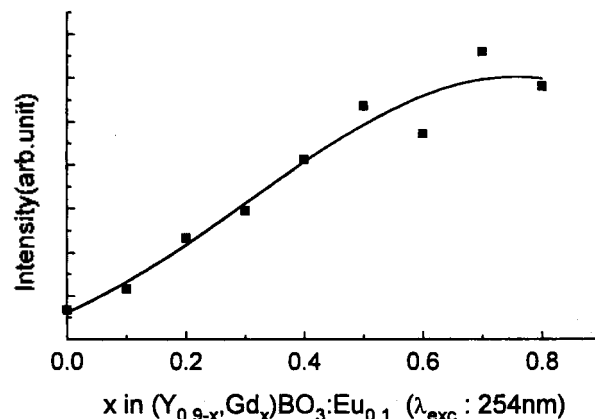


**Figure 3.** Luminescence intensity of  $Eu^{3+}$  (593 nm) of  $(Y_{0.9-x}Gd_x)BO_3:Eu_{0.1}$  as a function of Gd concentrations ( $\lambda_{exc}=254$  nm).

concentration of gadolinium maintains a low level. The phosphor,  $(Y, Gd)BO_3:Eu^{3+}$  has three intense luminescence lines at 593, 612 and 627 nm as shown in Figure 2. Relative intensities of emission lines at these wavelengths are plotted in Figure 4 as a function of europium concentrations with selective irradiations. Since a broad charge transfer band due to  $EuBO_3$  appears at 245 nm as shown in Figure 1, the irradiation at 255 nm which is within this band should affect intensities of emission lines at 593, 612 and 627 nm. Obviously emission intensities of these lines increase as europium concentrations increase as shown in Figure 4. Concentration quenching is observed at around 0.15 mole fraction of europium. Similarly the irradiation at 320 nm, corresponding to the direct excitation transitions within the  $4f^6$  configuration of  $Eu^{3+}$ , affects intensities of emission lines as shown in Figure 4. This confirms that 320 nm is indeed due to direct excitation of the  $Eu^{3+}$ . On the other hand the irradiation at 277 nm which corresponds to the transition of  ${}^8S_{7/2} \rightarrow {}^6I_{9/2} + {}^6I_{7/2}$  in  $Gd^{3+}$  shows different features. Emission intensities at 593, 612 and 627 nm are quickly saturated at concentrations below 0.05 mole fraction of europium. Above this limit, emission intensities do not much depend on europium concentrations. This suggests that all absorbed energy by gadolinium ions may be transferred to the europium ions and the  $Eu^{3+}$  luminescence intensities mainly depend on the concentration of gadolinium ions. The rate of energy transfer from gadolinium ions to europium ions seems to be slower than emission rate of europium ions. This may explain the constant emission intensities under irradiation at 277 nm. This behavior is further supported by the concentration dependence of the  $Eu^{3+}$  luminescence intensity on gadolinium ions as shown in Fig-

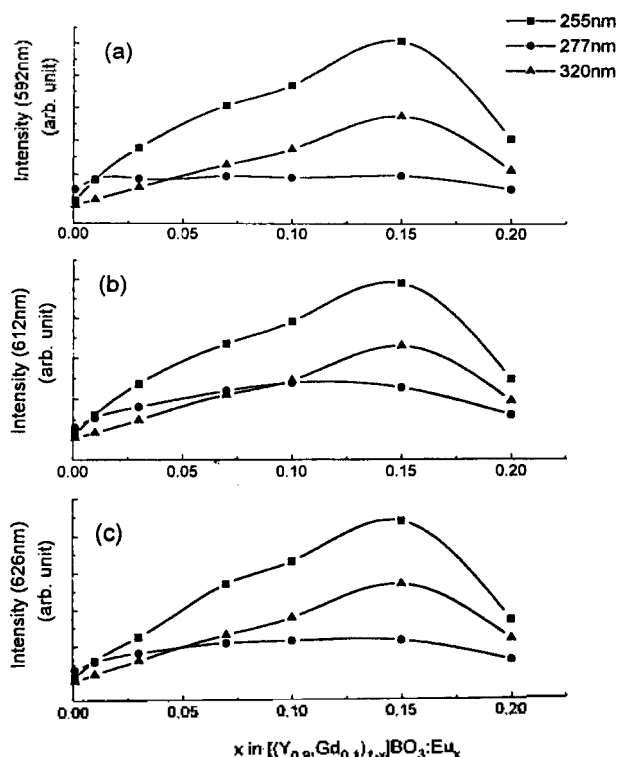


**Figure 4.** Luminescence intensity of  $Eu^{3+}$  of  $[(Y_{0.9}, Gd_{0.1})_{1-x}]BO_3:Eu_x$  as a function of  $Eu^{3+}$  concentrations.

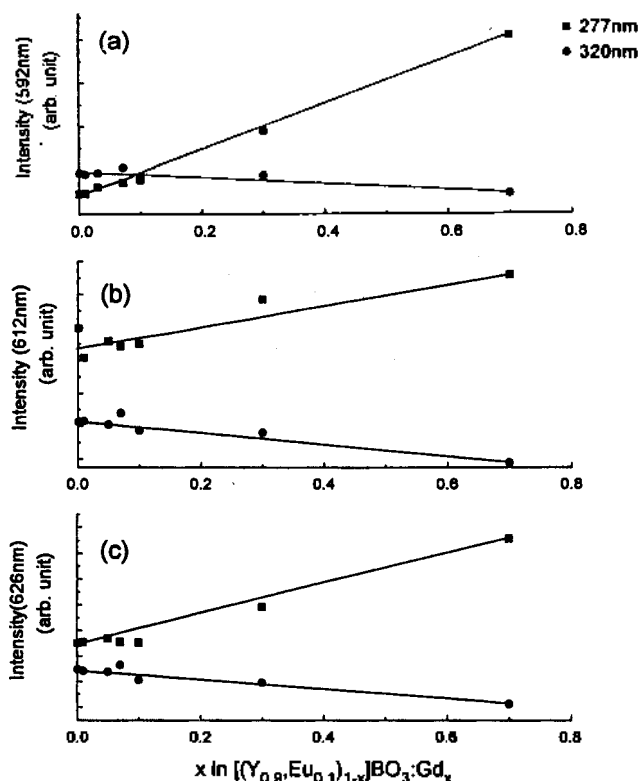


**Figure 5.** Luminescence intensity of  $Eu^{3+}$  of  $[(Y_{0.9}, Eu_{0.1})_{1-x}]BO_3:Gd_x$  as a functions of  $Gd^{3+}$  concentrations.

ure 2. If the energy transfer rate from gadolinium ions to europium ions is faster than emission rate of europium ions, the saturation due to gadolinium ions should occur in a low level of gadolinium concentrations.

In order to see the dependence of emission intensities on gadolinium concentrations under irradiation of direct excitation of the  $Gd^{3+}$  and the  $Eu^{3+}$ , the phosphors with the general formula  $[(Y_{0.9}, Eu_{0.1})_{1-x}Gd_x]BO_3$  ( $x=0.01-0.7$ ) were prepared. Figure 5 shows the variation of emission intensities as a function of gadolinium concentrations with selective irradiations. Emission intensities are increased as the concentration of gadolinium ion increases under irradiation at 277 nm as expected. This shows that the  $Gd^{3+}$  effectively transfers energy to  $Eu^{3+}$  in all investigated concentrations without a saturation due to a emission rate of europium ions. Emission intensities under irradiation at 320 nm are decreased slightly. This trend is explained in terms of a decrease in europium concentration.

**Acknowledgment.** This work has been supported by the Ministry of the Trade, Industry and Energy and the Ministry of the Science and Technology (G7 project). The authors also thank the solid state chemistry lab at KIST for helpful discussions and obtaining excitation spectra of this work.

## References

- A part of this work has been presented at the third International Display Workshops, November 27-29, 1996, Kobe, Japan
1. Weber, L. F. *Extended Abstract of the First International*

- Conference on the Science and Technology of Display Phosphors; p 23. November 14-16, 1995, Sandiego, California.
- Koike, J.; Kojima, T.; Toyonaga, R.; Kagami, A.; Hase, T.; Inaho, S. *J. Electrochem. Soc.: Solid-State Science and Technology* **1979**, *126*, 1008.
  - Lyuji Ozawa, *Cathodoluminescence-Theory and Applications*; VCH: 1990; Ch. 8., p 193.
  - Ropp, R. C. *Luminescence and the Solid State*; Elsevier: 1991; Ch. 8.

- Dean, J. A. *Langes's Handbook of Chemistry*, 13th Ed.; McGraw-Hill Book Company: New York, 1985.
- Ropp, R. C. *J. Electrochem. Soc.* **1965**, *112*, 181.
- Blasse, G.; Grabmaier, B. C. *Luminescent Materials*; Springer-Verlag: 1994; Ch. 3, p 41.
- Dexter, D. L.; Schulman, J. H. *J. Chem. Phys.* **1954**, *22*, 1063.

## Structural Study of 3,4-Bis(2-chlorophenyl)furazan N-Oxide and Speculation on the Fragmentation<sup>†</sup>

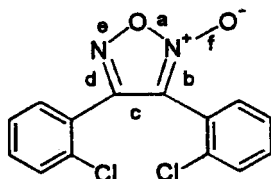
Seung Hee Lee, Inho Jo, Jae Hyun Lee<sup>§</sup>, and Kwang-Jin Hwang\*

Department of Industrial Chemistry, Hongik University, Jochiwon, Chungnam 339-800, Korea

<sup>§</sup>Korea Research Institute of Chemical Technology, P.O. Box 107, Yuseong, Taejon 305-606, Korea

Received April 15, 1997

The reactions for nitric oxide (NO) generation have been explored in regard to some biological activities: tumoricidal and bactericidal activities by macrophage,<sup>1</sup> a mediator of blood vessel relaxation,<sup>2</sup> and a signal transducing agent in neurotransmission in the brain.<sup>3</sup> In an effort of seeking NO precursors, several 3,4-disubstituted furazan N-oxides (furoxans) were prepared and confirmed to give nitric oxide by the fragmentations in mass spectrometer.<sup>4</sup> However, the high energy involved in electron-impacted fragmentation of a furoxan limited its application as a probe for NO-related physiology or a potential pharmaceutical agent for NO involved diseases. In an effort to release of NO by the fragmentation using relatively low energy, we have interested in the structure related fragmentation of the furoxan. Therefore, we studied carefully structural data of some furoxan derivatives. Here, we would like to report an X-ray crystal structure of 3,4-bis(2-chlorophenyl)furoxan (DCF, **1**), and any implication from the structure.



Structure 1

### Experimental

**Preparation and Measurements.** DCF was prepared as reported previously.<sup>4</sup> 2-Chlorophenyl nitrile oxide was dimerized after *in situ* generation by the reaction of the corresponding N-hydroxyiminoyl chloride with Et<sub>3</sub>N. It was recrystallized in hexane-EtOAc and confirmed by <sup>13</sup>C NMR (CDCl<sub>3</sub>), IR (KBr pellet), and elemental analysis. A Enraf-

Nonius CAD4/Turbo diffractometer equipped with a rotating anode generator and a graphite monochromator was used for preliminary experiments and for the subsequent collection of diffraction intensities, all at 294(1) K (Kyungpook National University). Preliminary experiment for the cell parameters and orientation matrix was carried out by least-squares methods, using the setting angles of 25 centered reflections. The structure was refined by full-matrix least-squares procedures. Crystal parameters and procedural information are in the Table 1. Final atomic coordinates and isotropic thermal parameters are given in Supplementary Material. The molecular structure of DCF is shown in Figure 1. Bond distances and angles are given in Table 2.

### Results and Discussion

Some comparisons between the bond distances of DCF and those of other furazan N-oxide derivatives are made as shown in Table 3. The O(1)-N(1) bond distance (1.44(2) Å) of DCF is similar to those of other derivatives, suggesting a more or less single bond character,<sup>5</sup> while the O(1)-N(2) bond distance (1.34(2) Å) is somewhat shorter than the corresponding bonds (1.367-1.406 Å) of other derivatives. The O(1)-N(1) bond (a in Table 3) is longer than the O(1)-N(2) bond (e). The difference between bonds a and e of DCF is approximately 0.10 Å, which is larger than those (0.010-0.077 Å) in most of other derivatives except in 3-Me-4-NO<sub>2</sub> furoxan. This fact may support that the bond a of DCF is more labile than the bond e (*vide infra*). The C(1)-C(2) bond distance (c, 1.44(2) Å) in DCF is somewhat longer than other furoxans except in 3-Br-4-adamantyl derivative (see Table 3). Since much of generalization with induction effect cannot be made,<sup>6</sup> this fact may be due to the steric hindrance. The N(1)-C(1) (b) and N(2)-C(2) (d) bond distances in DCF are 1.29(2) and 1.35(2) Å, respectively. This